

Drag coefficient modelling in the context of small launcher optimisation

Alexandru-Iulian ONEL^{*,1}, Tudorel-Petronel AFILIPOAE¹,
Ana-Maria NECULAESCU¹, Mihai-Victor PRICOP¹

*Corresponding author

¹INCAS – National Institute for Aerospace Research “Elie Carafoli”,
B-dul Iuliu Maniu 220, 061126, Bucharest, Romania
onel.alexandru@incas.ro*, afilipoae.tudorel@incas.ro, neculaescu.ana@incas.ro,
pricop.victor@incas.ro

DOI: 10.13111/2066-8201.2018.10.4.10

Received: 22 October 2018/ Accepted: 15 November 2018/ Published: December 2018

Copyright © 2018. Published by INCAS. This is an “open access” article under the CC BY-NC-ND license (<http://creativecommons.org/licenses/by-nc-nd/4.0/>)

Abstract: *The purpose of this paper is to present a fast mathematical model that can be used to quickly assess the drag coefficient for generic launcher configurations. The tool developed based on this mathematical model can be used separately or it can be integrated in a multidisciplinary optimisation algorithm for a preliminary microlauncher design.*

Key Words: *aerodynamics, drag coefficient, small launchers, multidisciplinary optimisation, mathematical model*

1. INTRODUCTION

The need for a small dedicated launcher emerged with the increased desire to insert into the Low Earth Orbit (LEO) of a growing number of nano - and micro- satellites. At the moment these payloads are carried into space as secondary payload in so-called “piggyback” missions. Because of the lack of dedicated small launchers, there are several ongoing projects worldwide that have as primary objective the development of a conceptual design for an affordable small launcher.

A multidisciplinary approach must be used to successfully obtain a preliminary design of the microlauncher, which is often realised with the aid of a multidisciplinary design optimisation (MDO) algorithm. The exact structure of the MDO algorithm can vary from one author to another. Figure 1 shows as an example the block scheme for the MDO algorithm used in the papers [1] and [2].

The MDO tool developed core is constituted by the four main disciplines that must be assessed: Weights & Sizing, Propulsion, Aerodynamics and Trajectory. The complexity of the last disciplines that must be integrated, in this case the trajectory, dictates the complexity of the entire MDO algorithm including the Aerodynamics module. To significantly reduce the complexity of each individual module of the MDO algorithm, a 3DOF approach is desired. As seen in [3] an accurate orbit injection is obtained even when using this simplified approach. For a more detailed overview of the launch vehicle conceptual design process, the papers [1] and [2] can be studied.

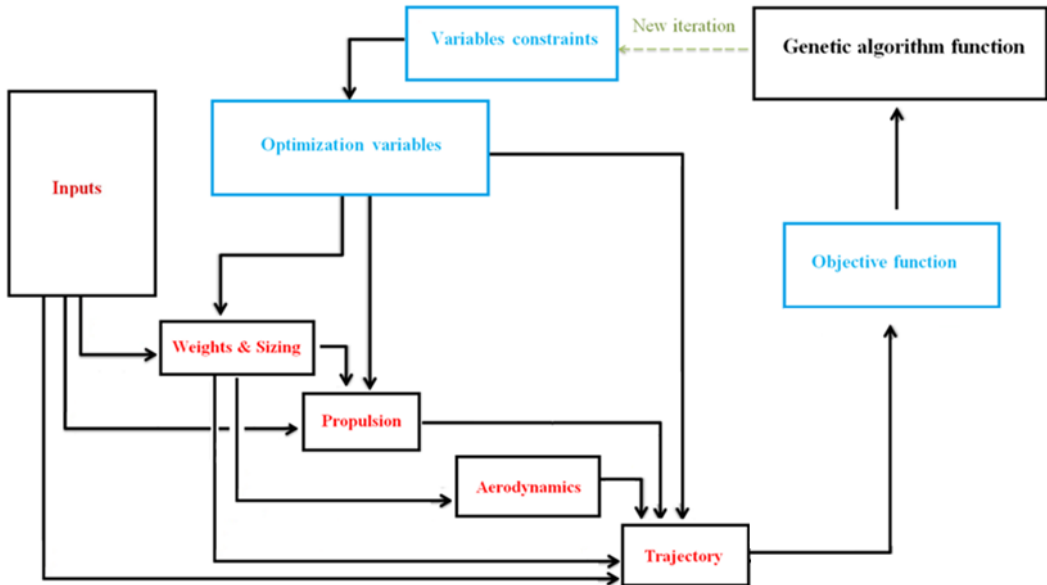


Figure 1 - Block scheme of a MDO algorithm

The objective of this paper is to elaborate the mathematical models that can be used in the aerodynamic assessment of the small launcher.

By using a 3DOF approach, the only aerodynamic assessment that must be realised is the estimation of the drag force acting on the launcher, which in the end, corresponds to computing the drag coefficient of the launcher at zero angle of attack.

2. DRAG ANALYSIS

The value of the drag force acting on the surface of the launcher is difficult to quantify because of the numerous factors that affect it. To get values that are suitable for comparison, the drag force (D) is normalised by the dynamic pressure (q) and the reference area (A_{ref}) to get a non-dimensional force coefficient. This is known as the drag coefficient and has the following definition:

$$C_d = \frac{D}{qA_{ref}} \quad (1)$$

The reference area used for the launcher is the maximum frontal area. The mathematical model used must provide accurate drag coefficient estimations for any possible small launcher configuration. Thus, it is practical to separate the launcher complex geometry into multiple simple geometric components. Such a breakdown can be seen in Figure 2.

$$C_{d_{launcher}} = \sum_i^N \left(\frac{A_i}{A_{ref}} \cdot C_{d_i} \right) \quad (2)$$

where: N - number of simple components; A_i - local reference area; C_{d_i} - individual component drag coefficient

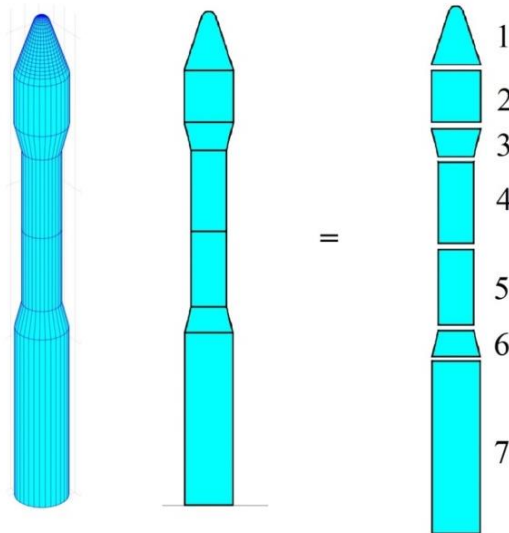


Figure 2 – Microlauncher breakdown into individual components

The methods used to assess the aerodynamic performance are based on linearized models and thus, the superposition principle can be applied. For each of the simple components, a drag coefficient will be calculated and normalized by the local reference area.

To compute the total drag coefficient of the launcher, all individual contributions are scaled to the global reference area and then summed up.

It is of interest to present what are the simple geometries that can be used to build up the studied launcher configurations. There are four major types of components, each one having its own mathematical model for the drag coefficient estimation.

The tool developed based on these mathematical models can use the following simple geometric components: Fairing – multiple nose cones; cylindrical stage; positive transition; negative transition. The simplest geometry can be imagined consisting of a fairing and a cylindrical stage, when the microlauncher stages have constant diameter.

A 2D view of some of the simple components used in the developed tool can be observed in Figure 3.

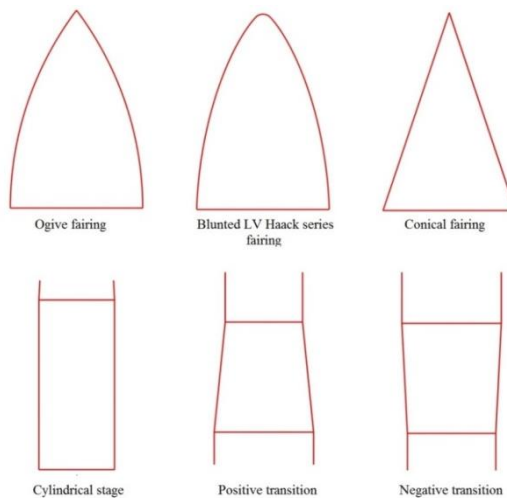


Figure 3 – Simple components used for aerodynamic assessment

Other components can also be used in the construction of the launcher. In some cases, the architecture of the launcher dictates that add-on boosters or fins are required. The necessity of adding fins to stabilise the launcher during the ascending phase has been removed because of the thrust vector controlling capabilities of the rocket motor. Also, when discussing small launchers, using boosters is not an optimal solution because the booster miniaturisation will not lead to a high enough performance to justify the price and mass increase. Also, the complexity of the launcher will be increased with the number of extra components which is not desired in the conceptual design phase.

Because the mathematical models have to provide very fast drag coefficient estimations, the launcher geometry is simplified, if needed. This is the reason why a skirt is added to the bottom part of the stage, zone where the nozzle is located.

The equations used to estimate the drag coefficient are based on both analytical and semi-empirical models. For each of the four main components (fairing, stage, positive transition and negative transition) different mathematical models are used to estimate the individual drag coefficient which will be presented in detail.

3. MATHEMATICAL MODEL

When calculating the drag coefficient for the launcher of interest, it is very important to first separate the drag into component parts. There are numerous methods of dividing the drag, as detailed in [4] the simplest being that of considering whether the drag is caused by normal acting forces to the launcher or by forces acting tangential to it. Here, the drag is divided into pressure drag and skin friction drag. The surface used to calculate the pressure drag is the launcher exterior geometry including the base.

Another method is to divide the drag into foredrag and base drag. The foredrag is considered to be all of the drag acting on the surface of the launcher excluding the base and contains both pressure and skin friction drag. The base drag is mainly due to pressure drag.

The last method that can be used is that in which the drag is divided into 3 main separate components. These are the pressure foredrag (also known as the body pressure drag), the base drag and the vicious drag (also known as the skin friction drag).

It is easier to consider that these components provide distinct quantities of drag but in reality, they are not independent of one another. The skin friction drag influences the base drag, but in this paper the 3 distinct quantities will be considered independent to reduce the complexity of the model.

Beside these 3 components of the drag, another one which is very difficult to quantify exists. Between the different components of the launcher interference drag can develop which can modify at least one of the 3 drag contributions. Interference drag mainly appears for configurations with add-on booster, which are not of interest for the current microlauncher study.

The aerodynamic drag, in this paper, for the case of the launcher, has thus 3 main contributions: Skin friction drag (C_{d_f}), body pressure drag (C_{d_p}) and base drag (C_{d_b}).

The individual drag coefficient is computed by summing all of the previous presented contributions:

$$C_{d_i} = C_{d_f} + C_{d_p} + C_{d_b} \quad (3)$$

The *skin friction drag* is caused by the friction between the vicious airflow and the launcher. In [5], the author presents equations for estimating the skin drag coefficient for both laminar and turbulent flow regimes.

For the case of interest of this paper, dealing with the size of the launcher and the high speeds occurring during the launcher ascent, it is safe to assume that the turbulent flow regime will be dominant for the most part; the laminar and transitional regime will appear only in the first seconds of flight.

To obtain the skin friction drag coefficient, one can use the following equation:

$$C_{df} = \begin{cases} C_f \cdot (1 - 0.1M^2) & , \text{if } M \leq 0.8 \\ \frac{C_f}{(1 + 0.15M^2)^{0.58}} & , \text{if } M > 0.8 \end{cases} \quad (4)$$

The skin friction coefficient (C_f) can be modelled as a function of Reynolds number (Re), the surface roughness (R_s) and launcher length (L). Papers [5] and [6] present a database with the surface roughness values based on the exterior surface type. Normal aviation paint has been considered for this paper.

The skin friction coefficient can be estimated using:

$$C_f = \begin{cases} \frac{0.664}{\sqrt{Re}} & , \text{if } Re \leq 5 \cdot 10^5 \\ \frac{0.455}{(\log_{10} Re)^{2.58}} - \frac{1700}{Re} & , \text{if } 5 \cdot 10^5 < Re \leq Re_{S.crit} \\ 0.032 \cdot \left(\frac{R_s}{L}\right)^{0.2} & , \text{if } Re > Re_{S.crit} \end{cases} \quad (5)$$

The skin friction coefficient is modelled adequately for each of the flow regime cases. In the laminar flow regime, the laminar flat plate approximation has been used, while for the transitional and turbulent regime, a model derived from the results of the turbulent flat plate has been used, together with the aid of a transition factor.

The most important regime in the case of a launcher is the “high” turbulent regime, where the surface roughness of the exterior surface is no longer inside the fully developed turbulent boundary layer. Thus, the skin friction drag is expected to be higher compared to a regular turbulent flow.

The surface roughness critical Reynolds number is defined as:

$$Re_{S.crit} = 51 \cdot \left(\frac{R_s}{L}\right)^{-1.039} \quad (6)$$

The local reference area used in the computation of the skin friction drag coefficient is the wetted area of the individual component. It is of great importance to correctly scale each of the drag contributions to the same reference area before adding them up to obtain the individual component drag coefficient (C_{d_i}).

The **body pressure drag** appears because the launcher is forcing the air to curve around it. This contribution of the total drag of the launcher occurs when modifications to the launcher geometry with respect to the airflow appear. The dominating component contribution for the pressure drag is the fairing, but it also appears at transitions or interstages. The problem of shock waves at supersonic and hypersonic speeds must be thoroughly investigated in detailed analyses, as the analytical and semi-empirical models offer only reasonable estimates. Several types of popular fairings will be now presented and the mathematical models used for estimating the pressure drag coefficient will be detailed.

The first geometry analysed is the conical fairing, where the nose pressure drag is proportional to the joint angle (ϕ), as derived from [7]. The joint angle for a conical fairing can be seen in Figure 4. The local reference area is that of the maximum frontal area which is proportional to the base diameter of the fairing.

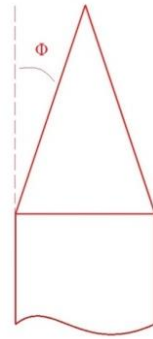


Figure 4 - Conical fairing joint angle

At very low speeds, the pressure drag coefficient can be estimated with:

$$C_{d_{p,M=0}} = 0.8 \cdot \sin^2 \phi \tag{7}$$

At a Mach number equal to 1, the pressure drag coefficient can be estimated with:

$$C_{d_{p,M=1}} = 1 \cdot \sin \phi \tag{8}$$

At supersonic speeds, for Mach numbers greater than 1.3, the pressure drag coefficient is provided in [8] and has the following form:

$$C_{d_{p,M \geq 1.3}} = 2.1 \cdot \sin^2 \phi + 0.5 \frac{\sin \phi}{\sqrt{M^2 - 1}} \tag{9}$$

The following equation will be used to estimate the pressure drag coefficient for Mach numbers lower than 1.3:

$$C_{d_p} = a \cdot M^b + C_{d_{p,M=0}} \tag{10}$$

where a and b are computed to fit the pressure drag coefficients from equations (7), (8), (9) and derivative constraints from [6].

For the ogive fairing, in the subsonic regime the pressure drag coefficient is small enough to be negligible, while in the transonic and supersonic regimes, the ogive pressure drag coefficient is computed using an analogy with the conical fairing, where the pressure drag coefficient is corrected with the shape factor:

$$C_{d_p} = \left(0.72 \cdot (\kappa - 0.5)^2 + 0.82\right) \cdot C_{d_{cone}} \quad (11)$$

The ogive shape parameter (κ) of 1 corresponds to a tangent ogive and values between 0 and 1 will result in a secant ogive.

For other types of fairing, analytical models are not capable of accurately estimating the pressure drag. For the next fairings semi-empirical models will be used.

One of the most accurate fairing databases is the one in [9], database which will be the starting point of the mathematical model used to assess the fairings pressure drag coefficient.

The drawbacks of the database are that it only contains results for nose fineness ratio 3 and also for Mach number up to 2. The most popular fairings are the Haack series type because they are not geometrical derived, but rather mathematically derived to minimise drag. The L-D Haack series, also known as the von Kármán ogive has the minimal drag but is somewhat restrictive on the interior volume.

For a greater interior space, suitable for mounting satellites, with a small increase in drag, the L-V Haack series is preferred.

Based on this database, semi-empirical model has been developed and some of the results can be observed in Figure 5.

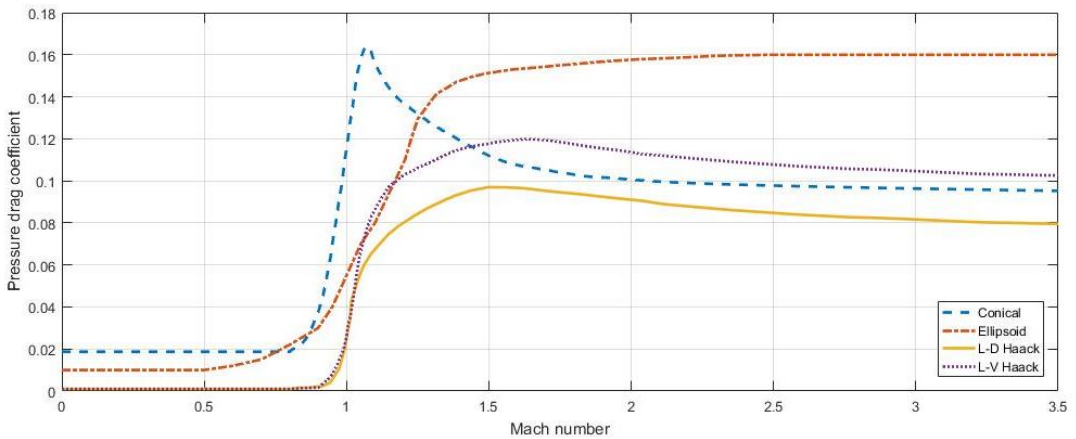


Figure 5 – Fairing pressure drag coefficient, from [9]

It is now of interest to expand the model for other fairing fineness ratio. The fineness ratio is defined as:

$$f_N = \frac{L_{fairing}}{D_{fairing}} \quad (12)$$

Here, the diameter is considered to be the base diameter of the fairing. For a fairing having $f_N = 0$, the data from a blunt cylinder can be used, where the pressure drag coefficient is proportional to the stagnation pressure, as stated in [8].

$$C_{d_p, f_N=0} = 0.85 \cdot \frac{q_s}{q} \tag{13}$$

$$\frac{q_s}{q} = \begin{cases} 1 + \frac{M^2}{4} + \frac{M^4}{40} & , \text{if } M \leq 1 \\ 1.84 - \frac{0.76}{M^2} + \frac{0.166}{M^4} + \frac{0.035}{M^6} & , \text{if } M > 1 \end{cases} \tag{14}$$

Having now the pressure drag coefficient for two different fineness ratios (0 and 3), the following approximation can be used for the pressure drag coefficient estimation:

$$C_{d_p} = \frac{a}{(f_N + 1)^b} \tag{15}$$

After simple calculations it can be observed that:

$$\begin{cases} a = C_{d_p, f_N=0} \\ b = \log_4 \left(\frac{C_{d_p, f_N=0}}{C_{d_p, f_N=3}} \right) \end{cases} \tag{16}$$

In most cases, for thermal loads decrease during the launcher ascent purposes, the nose is not sharp at the tip, but rather blunted. The bluntness ratio (B_r) is defined as:

$$B_r = \frac{R_n}{R_f} \tag{17}$$

where: R_n - nose radius; R_f - fairing base radius.

The top part of the fairing is now a sphere, a tangency condition being used at the junction between the fairing profile and the spherical tip. Because of the rounding of the top part of the fairing, its total length will decrease with the increase of the bluntness ratio, as shown in Figure 6 for different fairing profiles.

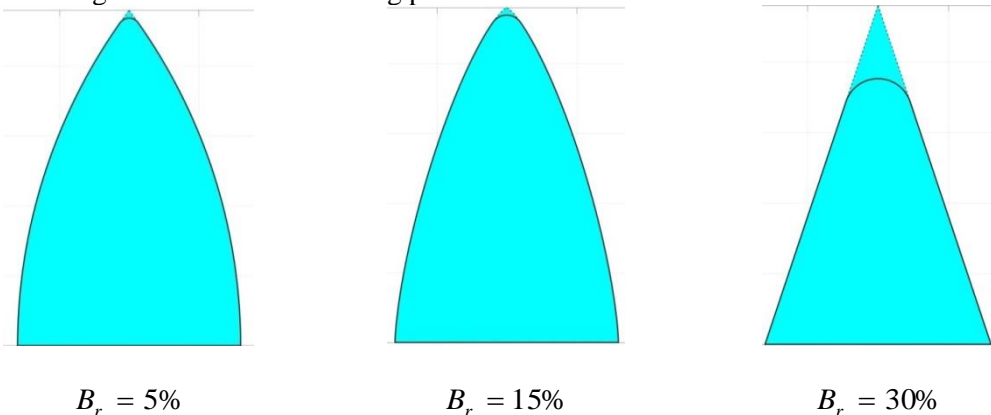


Figure 6 – Nose bluntness ratio comparison

Using a blunted nose also has an impact on the pressure drag coefficient. If the bluntness ratio is below a threshold then the increase in drag is not significant. This threshold is in the range of 15% - 20%, as stated in [9], [10] and [11]. It is thus advised to limit the bluntness ratio to 15% in order not to significantly increase the launcher drag coefficient, while still decreasing the thermal loads on the fairing.

The following relations are proposed to compute the effect of the tip bluntness:

$$C_{d_{p,blunt}} = C_{d_{p,sharp}} \cdot F_{c,r} \quad (18)$$

$$F_{c,r} = 1 - 0.16 \cdot B_r + 4.6 \cdot B_r^2 \quad (19)$$

For the cylindrical stages the pressure drag coefficient is negligible because there are no modifications in the geometry with respect to the airflow. For positive transitions, an analogy with the conical fairing is made. The pressure drag coefficient is considered to be the same as for a cone having the same joint angle, the local reference area being the difference between the aft and fore ends of the transition.

In the case of negative transitions, the proposed model is based on wedges data. The pressure drag coefficient for a negative inter-stage or boat tail can be estimated using:

$$C_{d_p} = \beta \cdot \frac{A_{fore}}{A_{aft}} \cdot C_{d_{b,aft}} \cdot \begin{cases} 1 & , \text{if } \sigma \leq 1 \\ \frac{3 - \sigma}{2} & , \text{if } 1 < \sigma \leq 3 \\ 0 & , \text{if } \sigma > 3 \end{cases} \quad (20)$$

$$\beta = \begin{cases} 0 & , \text{if } M \leq 0.8 \\ 1 & , \text{if } M > 0.8 \end{cases} \quad (21)$$

where: σ - length to height ratio for the negative transition ($\sigma = \frac{\text{length}}{d_{fore} - d_{aft}}$); $C_{d_{b,aft}}$ - equivalent base drag coefficient for the aft part of the transition.

The length to height ratio of 1 corresponds to a 27° reduction angle and the height to length ratio of 3 corresponds to a 9° reduction angle for the negative transition. If negative transitions are to be used in the small launcher architecture it is thus desired that they have a very small reduction angle.

The **base drag** occurs when a low pressure area is created at the end/base of the launcher or in any place where the body diminishes rapidly. It is the most difficult drag contribution to quantify because it is highly dependent on the flow separation point. Also it is directly influenced by the exhaust gases.

Paper [11] suggests using a single relation based on tactical missiles for the base drag coefficient estimation, but the accuracy of the results provided is low. In [9], the author presents a theoretical distribution of the base drag coefficient for a three dimensional body of

revolution for a specific Mach number interval. In [12] experimental results of interest can be gathered, for supersonic flow conditions. In this paper a hybrid model based on the results from [9] and [12] is chosen. The data used are from different Mach intervals. Between the two sets of data, a matching curve model is proposed for $0.8 < M < 1.5$, being similar to the theoretical distribution, only adjusted with a correction factor of 1.2. The proposed model base drag distribution is presented in Figure 7, together with the data from [9] and [12]. For Mach numbers greater than 10, the data from [12] have been extrapolated and a simplified equation is provided in (22).

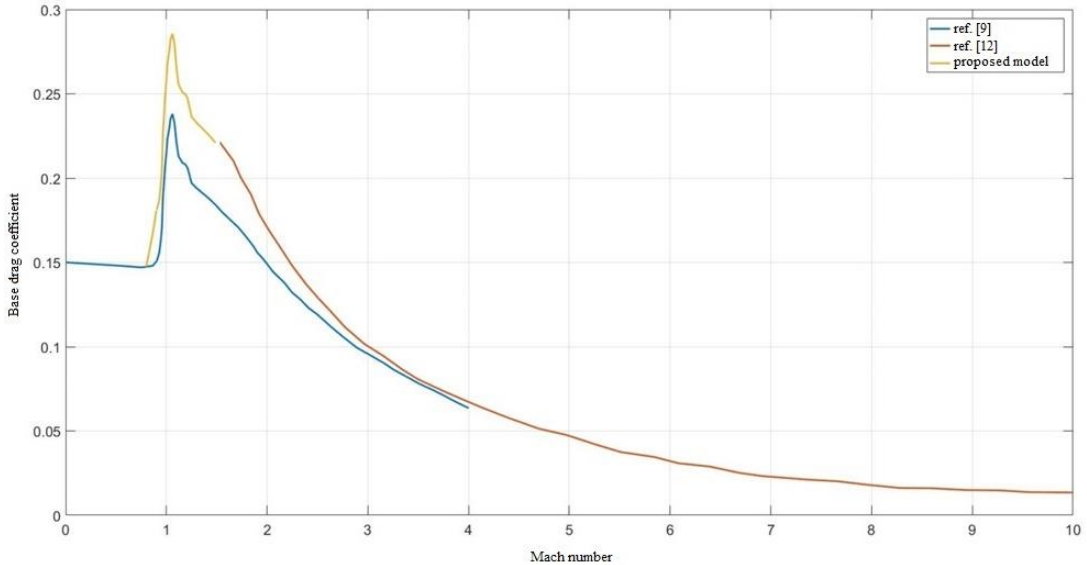


Figure 7 – Base drag coefficient model

Summarising, the following data are used for the base drag coefficient computation:

$$C_{d_b} = \begin{cases} \text{ref.}[9] \text{ model} & , \text{if } M \leq 0.8 \\ \text{proposed model} & , \text{if } 0.8 < M < 1.5 \\ \text{ref.}[12] \text{ model} & , \text{if } 1.5 \leq M < 10 \\ \frac{0.13}{M} & , \text{if } M \geq 10 \end{cases} \quad (22)$$

The local reference area for the base drag computation is that of the aft end, which is in many cases, also the global reference area. The exceptions are that of launchers with a wider fairing than the base, used to encapsulate voluminous payloads.

The influences of the exhaust gases are very difficult to quantify by means of analytical or semi-empirical formulations. As stated in [6], in a simplified model it can be considered that the reference area for the base drag is reduced by the exhaust exit area when the rocket motor is in operation. For a detailed analysis, CFD investigations are required, but they are not needed in the preliminary design of the launch vehicle. In this paper, the influence of the exhaust jet will not be considered, thus the studied configuration is the one that appears in the coasting phase of the trajectory (also known as the power-off configuration).

Another important aspect of the launcher geometry is whether the launcher nozzles are in a streamlined enclosure, such as an engine/nozzle skirt or not. If the nozzles are exposed then in that region recirculation pockets can occur, especially at low speeds, which are very hard to predict and to quantify in a drag coefficient.

It is preferred to have this in mind when using the MDO approach and if the nozzles are not enclosed by a skirt then a simplification of geometry is needed so that the mathematical model presented can be applied.

For a fast, first approximation of the drag coefficient the models presented in this paper offer good results and have the advantage of being robust enough so the majority of small launcher geometries can be calculated.

4. RESULTS

Based on the mathematical model earlier presented, a Matlab tool has been developed. The average run time for a 3-stage small launcher is around 0.02sec.

This small computational time is desired because when implemented in a full loop MDO tool, for the optimal solution to reach convergence it can take up to several hundred thousand iterations [2].

For this paper, sea level conditions have been used, for both the Matlab tool and the CFD investigations.

To validate the results provided with the mathematical model proposed in this paper, a comparison with CFD results, obtained with the aid of Ansys Fluent, version 18 is used. The microlauncher test geometry proposed can be observed in Figure 8, while details about its dimensions are presented in Table 1.

The microlauncher geometry is a complex one, having in its architecture both positive and negative transitions.

Table 1 – Test configuration dimensions

Test configuration	
Component	Dimensions
Fairing	Length: 2.4m/1.65m/0.9m
	Diameter : 1.6m/1.15m
	LD Haack nose cone
Third stage	Length : 2.6m
	Diameter: 1.15m
Second stage	Length : 2.4m
	Diameter: 1.15m
Interstage 1-2	Length : 0.8m
	Fore diameter: 1.15m
	Aft diameter: 1.55m
First stage	Length : 5.5m
	Diameter: 1.55m

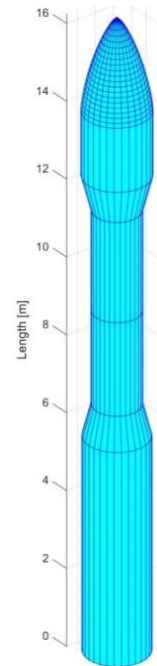


Figure 8 – Test configuration

The results obtained with the aid of the model proposed in this paper are shown in Figure 9 and Figure 10.

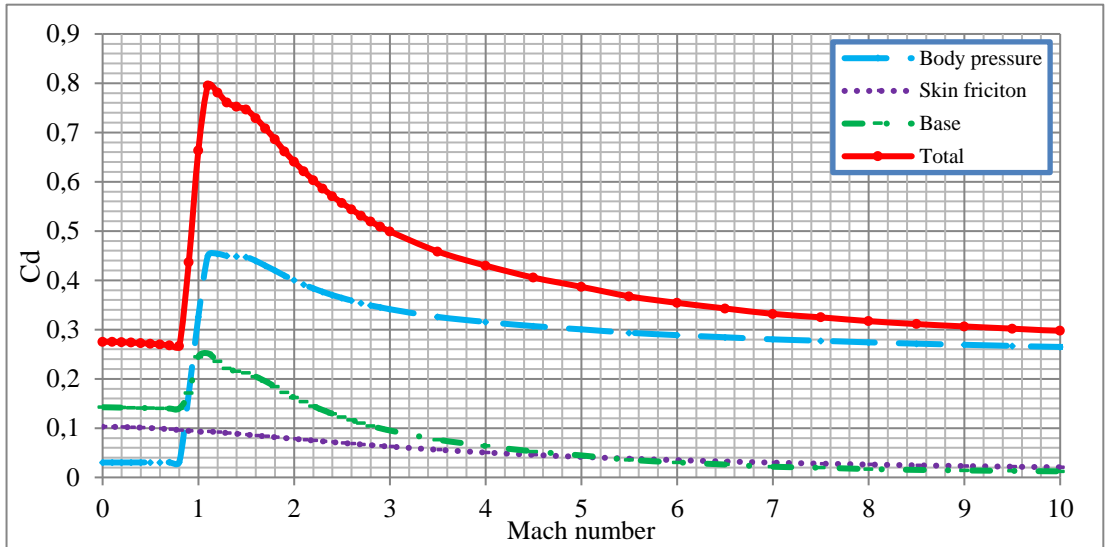


Figure 9 – Drag coefficient contributions

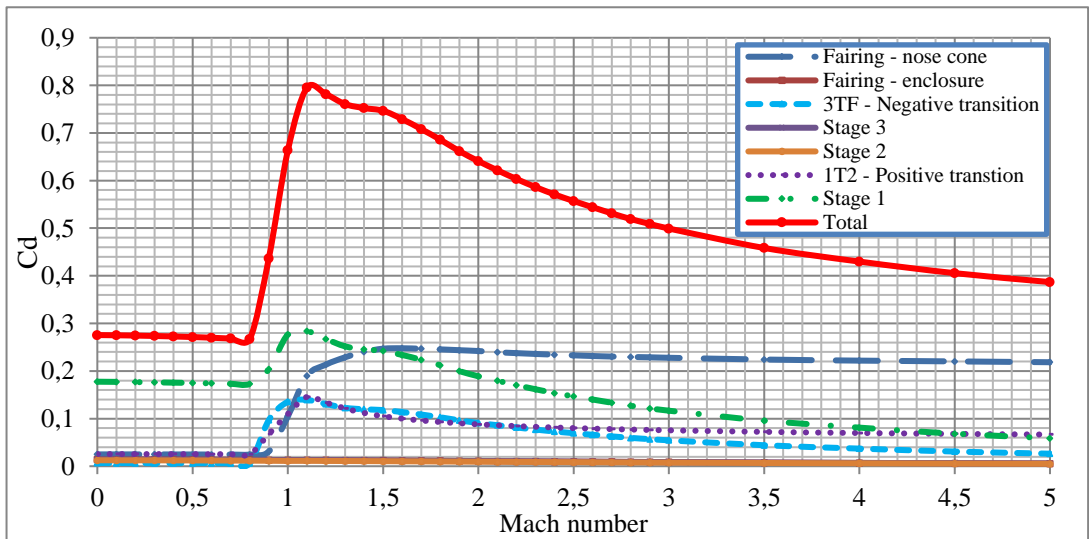


Figure 10 – Individual components drag

In Figure 9 the launcher drag coefficient variation with Mach number can be observed for all of its contributions, up to Mach 10.

In the subsonic region, the most important drag contribution is that of the base drag, but after passing the Mach 1 mark, the dominant contribution is that of the body pressure drag. A steady decrease in friction drag can also be observed as the Mach number increases, being almost one order of magnitude lower than the pressure drag at very high speeds.

Figure 10 depicts the contribution of all of the 7 individual components composing the launcher complex geometry.

Only 4 of these 7 components generate significant drag: the launcher nose cone, the two transitions and the first stage.

Again, it can be seen that in the high supersonic flow regime, the dominant drag contribution is given by the fairing nose cone which is responsible for the apparition of body pressure drag.

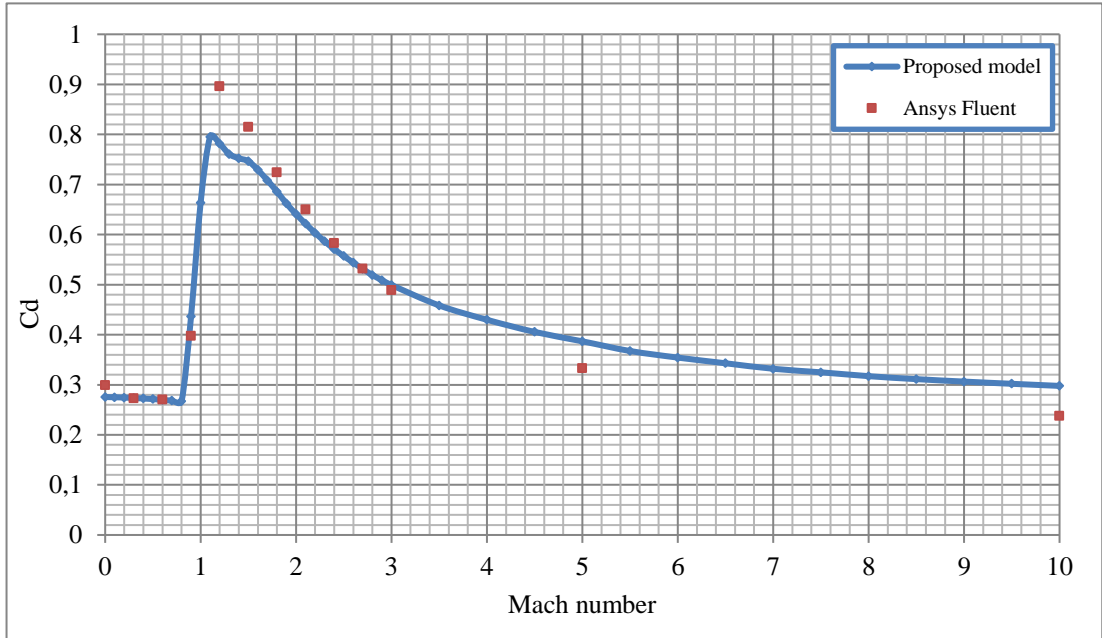


Figure 11 – Comparison with CFD

Figure 11 shows the results provided by the proposed model and the ones obtained with the aid of CFD techniques. A high order of accuracy has been obtained, the computational time needed for the tool developed being only a very small fraction of the one needed for the CFD computations.

5. CONCLUSIONS

The paper presents a mathematical model based on analytical and semi-empirical aerodynamic assessment methods. The proposed model can be used to quickly assess the drag coefficient for most small launcher configurations.

In the preliminary phases of a launcher design, when a high number of configurations must be quickly aerodynamically assessed, the models providing fast approximations are preferred. In this paper, the launcher is divided into individual simple geometric components which are then aerodynamically assessed via drag coefficient estimation. To compute the launcher total drag coefficient the individual contributions are scaled to the reference area and then summed up.

The results provide a very good first approximation, as can be seen from the comparison with the CFD results. The tool developed based on this mathematical model can be used separately or it can be integrated in a more complex, multidisciplinary optimisation tool. Because of the low computational time, the proposed mathematical model is suitable to be used in a full loop MDO algorithm.

REFERENCES

- [1] T. P. Afilipoae, A. M. Neculăescu, A. I. Onel, M. V. Pricop, A. Marin, A. G. Perșinaru, A. M. Cișmilianu, I. C. Oncescu, A. Toader, A. Sirbi, S. Bennani, T. V. Chelaru, Launch Vehicle - MDO in the development of a Microlauncher, *Transportation Research Procedia*, vol. **29**, Pages 1-11, 2018.
- [2] A. I. Onel, T. P. Afilipoae, A. M. Neculăescu, M. V. Pricop, *MDO approach for a two-stage microlauncher*, *INCAS Bulletin*, ISSN 2247-4528, vol. **10**, issue 3, pp. 127-138.
- [3] T. V. Chelaru, A. I. Onel, A. Chelaru, *Microlauncher, mathematical model for orbital injection*, *International Journal of Geology*, vol. **10**, ISSN: 1998-4499, 2016.
- [4] J. N. Nielsen, *Missile Aerodynamics*, Nielsen Engineering & Research, IN., Mountain View, California, 1988.
- [5] J. Barrowman, *The practical calculation of the aerodynamic characteristics of slender finned vehicles*, M.Sc. thesis, The Catholic University of America, 1967.
- [6] N. Sampo, *OpenRocket technical documentation*, Available at www.openrocket.info, 2013.
- [7] * * * United States, Bureau of Naval Weapons., Handbook of supersonic aerodynamics, Section 8, *Bodies of revolution*, Navweps Report 1488, 1961.
- [8] S. F. Hoerner, *Fluid-dynamic drag*, published by the author, 1965.
- [9] W. Stoney, *Collection of Zero-Lift Drag Data on Bodies of Revolution from Free-Flight Investigations*, *NASA-TR-R-100*, 1961.
- [10] S. S. Chin, *Missile Configuration Design*, 1961.
- [11] E. Fleeman, *Tactical missile design*, 2nd edition, p. 33, AIAA, 2006.
- [12] C. S. James, R. C. Carros, *Experimental investigation of the zero-lift drag of a fin-stabilized body of fineness ratio 10 at Mach numbers between 0.6 and 10*, NACA RMA53D02.